

© 1980 IEEE. Personal use of this material is permitted. However, permission to reprint/republish this material for advertising or promotional purposes or for creating new collective works for resale or redistribution to servers or lists or to reuse any copyrighted component of this work in other works must be obtained from the IEEE.

This material is presented to ensure timely dissemination of scholarly and technical work. Copyright and all rights therein are retained by authors or by other copyright holders. All persons copying this information are expected to adhere to the terms and constraints invoked by each author's copyright. In most cases, these works may not be reposted without the explicit permission of the copyright holder.

EXPERIMENTAL MEASUREMENT OF THE LOW ANGLE
TERRAIN SCATTERING INTERFERENCE ENVIRONMENT

J. E. Evans
D. F. Sun

M.I.T. Lincoln Laboratory

ABSTRACT

This paper presents the results of an experimental program to obtain a better quantitative understanding of low angle microwave propagation phenomena needed to assess the potential for improved elevation tracking performance. It has long been recognized that terrain multipath (e.g., reflections and/or shadowing) are a principal limitation on the achievable accuracy of radar elevation trackers and/or landing navigation aids at low angles; however, there has been a paucity of relevant experimental data over irregular terrain.

The experimental data presented were obtained with a 26λ L-band array and a 57λ C-band array at a variety of sites in eastern Massachusetts with vegetated and/or rolling terrain. It is shown that specular reflections appear to be the predominant multipath source and these are predictable from a model based on scattering from tilted plates.

I. INTRODUCTION

Figure 1-1a illustrates the propagation phenomena of interest in low angle tracking [1,2]. Since elevation tracker antennas generally have quite directional patterns in the elevation plane, a critical factor in refining and predicting the performance of an elevation tracker is the distribution of the received signal power as a function of elevation angle (i.e., the so-called angular power spectrum) [1]. Figure 1-1b illustrates the angular power spectrum that might arise with the multipath environment shown in Fig. 1a. We treat the problem of multipath environment characterization as one of estimating the angular power spectrum of the received signal.

The approach taken here is based on adaptive processing of the received aperture information. Our goals are (1) to obtain higher resolution angular power spectrum than would be obtainable

This work was sponsored by the Federal Aviation Administration. "The views and conclusions contained in this document are those of the contractor and should not be interpreted as necessarily representing the official policies, either expressed or implied, of the United States Government."

with the "conventional" beam sum spectrum, and (2) to correlate the measured results with the propagation model [16] developed for Microwave Landing System (MLS) multipath simulations. The starting point in our approach is measuring the (complex) received waveform (i.e., the amplitude and phase) at various points along the receiving antenna aperture. Next, we apply several high resolution spectral analysis techniques to the spatial sample data. Here, specifically, we consider the use of the maximum likelihood (ML) and the maximum entropy (ME) spectral estimation methods which have been applied in time series analysis and seismic/sonar array processing [3-6] for resolving closely spaced spectral lines.

The remainder of the paper is organized as follows. Section II briefly describes the high resolution algorithms employed in our work and shows some examples of applying them to synthetic data. These algorithms are then used in analyzing field data from an L- and C-band terrain reflection measurement program. These experimental results and corresponding propagation model estimates are presented in Section III, followed by the summary of the results in the last section.

II. HIGH RESOLUTION SPECTRUM ESTIMATION
PROCEDURES

There has been much discussion of the maximum likelihood (ML) and the maximum entropy (ME) techniques recently in the geophysics and time series analysis literature.[†] The notational convention we will use is that column vectors or matrices are represented by underlined lower-case letters. The asterisk denotes the conjugate transposition. Underlined uppercase letters represent Hermitian matrices. Thus, vector \underline{s} represents the complex sensor outputs of the line array, while the covariance matrix \underline{R} has as its i, j th entry $R_{ij} = \langle \underline{s}_i \underline{s}_j^* \rangle$. The spatial samples are taken at points $x_k = j_k \delta$, where δ is the sensor spacing in wavelength.

The ML technique had its genesis in seismic array beamforming under conditions of directional interference [3] and adaptive array nulling of incoherent interfering sources [7]. The problem is formulated as determining the minimum variance unbiased estimate of the power from a given angle

[†]Reference [14] contains many relevant papers.

subject to the interference (complex) covariance matrix. If the interference were Gaussian with a known covariance matrix \underline{Q} (e.g., via measurements in the absence of the desired signal), the maximum likelihood estimate of the power in a plane wave from angle θ would be given by

$$P_{ML}(\theta) = \underline{e}^* \underline{Q}^{-1} \hat{\underline{R}} \underline{Q}^{-1} \underline{e} / (\underline{e}^* \underline{Q}^{-1} \underline{e})^2 \quad (1)$$

where $\underline{e} = \exp(j2\pi x_k \sin \theta)$ is the received signal vector corresponding to a unit plane wave from angle θ and $\underline{R} = \underline{s} \underline{s}^*$ is the raw sample covariance matrix.

Unfortunately, when the interfering signals are multipath and/or coherent jammers, \underline{Q} cannot be measured independently of the desired signal. Capon [3] suggests using the \underline{R} as an estimate of \underline{Q} , so that the ML angle power spectrum estimate is then given by

$$P_{ML}(\theta) = (\underline{e}^* \hat{\underline{R}}^{-1} \underline{e})^{-1} \quad (2)$$

The estimate (2) may be contrasted to the standard "beam sum" (BS) angle power spectrum estimate of

$$P_{BS}(\theta) = |\underline{e}^* \underline{s}|^2 = \underline{e}^* \hat{\underline{R}} \underline{e} \quad (3)$$

This particular BS estimate gives rise to a sin K θ /K θ beam pattern which has a high sidelobe level (-13 dB). By weighting the data samples, lower sidelobes are obtained at the "cost" of wider beamwidths (i.e., poorer resolution).

The use of the ME technique for high resolution spectrum estimation has been justified by a variety of arguments [4-6]. The physically most meaningful argument for radar applications is that the received angular spectrum can be represented by a finite number of poles in the complex plane, i.e.,

$$e(\theta) = P_E / |\sum a(k) z^{-k}|^2 \quad (4)$$

where $z = \exp(j 2\pi \delta \sin \theta)$ and the roots z_1 of the denominator polynomial lie on or within the unit circle. The case of z_1 on the unit circle corresponds to discrete plane waves, while z_1 inside the unit circle might correspond to an extended target (e.g., diffuse reflections). Time samples with the spectrum of (4) may be generated by passing a white noise process through an all pole filter of order N , which is a standard model in autoregression (AR) time series analysis. The duality between space and time [15] allows us to utilize many AR results.

The observed antenna sample data can be considered as 1) a deterministic signal (with unknown parameters) which is corrupted by additive noise, or 2) a spatially nonstationary sample function from a random process. Recent work by Lan [8,9] has shown that the most appropriate ME estimation technique for this case is the "modified covariance" technique of Urych and Clayton [10], whereby the model coefficients a are determined by directly minimizing forward and backward

prediction error energies.[†] This particular algorithm can be shown to be substantially better in terms of spectrum resolution and angle of arrival estimation than the more common Yule-Walker (autocorrelation) [11] and Burg [5] techniques when the observed signal is a sum of plane waves in noise. When in addition, a least squares fit is used to determine the amplitudes of the plane waves associated with a spectrum peak [9], the resulting estimates of plane wave angle of arrival and amplitude approach the Cramer-Rao bounds for the true ML estimate [12].

The "modified covariance" mathematical formulation leads to an implied covariance estimate

$$\phi(m, k) = \frac{1}{Z(N-P)} \left[\sum_{n=P}^{N-1} \hat{R}_{n-m, n-k} + \sum_{n=0}^{N-P-1} \hat{R}_{n+k, n+m} \right] \quad (5)$$

where P = maximum index of k in Eq. (4) and N is the number of array elements. The covariance estimate given by (5) is used in Eq. (2) to yield the ML spectrum estimate. This is equivalent to dividing the array into $N-P$ overlapping subapertures of length P and averaging the respective raw covariances.

Figure 2-1 shows the results of applying these techniques to synthetic data consisting of two plane waves with independent noise added to each spatial sample. The actual angular power spectrum consists of impulse functions at the plane wave angles. The example given is a case where the components are too close (0.50 standard beamwidths) with an unfavorable relative rf phase (0°) to be resolved by classical methods. In this particular case, only the ME method gives an estimate close to the actual spectrum. At higher SNR or greater plane wave angular separations, the ML method would also be successful.

III. EXPERIMENTAL RESULTS

Figure 3-1 shows the aperture sampling equipment utilized in the field measurements. The L-band sampled aperture consisted of a 5-element 6.5λ array (for evaluation of small aperture tracker performance) as well as a 9-element 26λ line array (for fine grain resolution of various multipath components). The C-band line array has 21 lower elements with a 1.6λ spacing and 9 upper elements with a 3.2λ spacing. The received L-band signal consists of 1090 MHz replies from a standard air traffic control radar beacon (ATCRB) on board an helicopter in response to the ground interrogations, while the C-band CW signal is obtained from a TWT. The amplitude and phase* of the received signal at each array element are digitized and recorded on magnetic tape. Also recorded are the elevation angle of the helicopter

[†] i.e., the is not an intermediate step in which one attempts to estimate the autocorrelation function of the data [11,13].

*The RF phase was measured relative to a reference dipole, while the amplitude was measured on calibrated log video receivers.

obtained from a tracking theodolite as well as various environmental data.

The received signal consists of a plane wave at positive elevation angle (corresponding to the direct signal coming from the aircraft) and other plane waves generally at negative elevation angles (corresponding to various ground reflections from terrain features). Thus, as shown in Fig. 1-1, we expect that the angular power spectrum of the received signal (i.e., the received signal power as a function of elevation angle) will consist of a narrow peak at the direct signal elevation angle, narrow peaks at the arrival angles of the major specular ground reflections, and wider peaks in regions of diffuse scattering [1].

Figure 3-2 shows the experimental angular power spectral estimates for a special measurement at MIT Lincoln Laboratory antenna test range where the elevation array was laid sideways horizontally on the ground and signals transmitted from two laterally displaced antennas 2000 feet away. The results are seen to correspond closely to the synthetic data result of Fig. 2-1 and are viewed as providing a degree of validation for our data recording and analysis procedure.

Ground reflection field measurements were made for various terrain conditions. Results for both near-flat terrain and rolling terrain are given below. For comparison purposes, both the experimental angular power spectral estimates from the field measured data and the corresponding simulated spectral estimates (using the multipath computer simulation program developed for the Microwave Landing System multipath simulations [16]) are shown in the same figure.

Figure 3-3a shows the L-band angular power spectral estimates for a flight test in which the target helicopter was at an angle of 2° and at a range of 0.4 nmi. Figure 3-3b gives the corresponding C-band result. Figure 3-4 shows the terrain height profile and the corresponding ground model used to generate the simulated spectral estimates. The terrain in front of the receiving antenna array consisted of a fairly flat grass field adjacent to the main runway at Hanscom airport, Mass. Thus, it is expected that the ground reflected signal would be primarily a specular reflection from the fairly flat ground which has been attenuated by the grass cover. For the L-band data, in both measured and simulated results, it can be seen that all three angular power spectral estimates suggest the presence of two signals (one direct signal and one ground reflected signal). The indicated arrival angle of the ground reflected signal can be explained very well by the flat ground reflection together with the downward sloping of the ground in front of the receiving array as shown in Fig. 3-4. Both measured and simulated C-band results show more ground reflections than the L-band data; however, in both L-band and C-band results, high specular reflection levels around -1 dB and -3 dB were observed.

Figures 3-5a (L-band) and 3-5b (C-band) show the spectral estimates for a flight test in which the target helicopter was at 4.2° and 0.6 nmi. This field test was taken at the golf course at Fort Devens, Mass. Figure 3-6 shows the terrain height profile and the corresponding ground model used to produce the simulated spectral estimates. Here, the terrain in front of the receiving antenna array has various downward and upward slopes within a roughly level horizon and the ground was covered uniformly by short grass. This type of rolling terrain can often give rise to the "focusing" terrain reflections, i.e., more than one specular reflection presented at a given time. For the L-band data, we see that both the field measured result and the simulation result indicate the existence of the two ground reflected signals, one at -6.0° and the other at -2.5° with the latter having lower multipath level. The corresponding C-band result again shows more specular ground reflections, as we saw previously. However, here the C-band result indicates much lower multipath level than the L-band result. Additional examples of terrain reflection and diffraction phenomena are presented in [17].

IV. SUMMARY

Our preliminary results from analysis of the low terrain scattering field measurements by utilizing the high resolution spectral estimation field techniques suggest that these modern spectral estimation methods, especially the ME method, can be effectively used for ground reflection elevation multipath characterization. The angular spectra observed to date can be qualitatively and quantitatively predicted by a model based on specular reflections from tilted flat plates. The number of specular reflections at higher microwave frequencies (e.g., 5 GHz) were substantially larger in number than the corresponding results at the same site at lower microwave frequencies (1 GHz).

REFERENCES

1. D. Barton, "Low-Angle Radar Tracking", Proc. of IEEE, p. 687, June 1974.
2. W.D. White, "Low Angle Radar Tracking in the Presence of Multipath", IEEE Trans. on AES, Vol. AES-10, No. 6, p. 835, November 1974.
3. J. Capon, "High-Resolution Frequency-wave Number Spectrum Analysis", Proc. of IEEE, Vol. 57, p. 1408, August 1969.
4. R.T. Lacoss, "Data Adaptive Spectral Analysis Methods", Geophysics, Vol. 56, No. 6, p. 661, August 1971.
5. J.P. Burg, "Maximum Entropy Spectral Analysis", paper presented at 37th International SEC Meeting, Oklahoma City, Oklahoma, October 1967.
6. A. Van Den Bos, "Alternative Interpretation of Maximum Entropy Spectral Analysis", IEEE Trans. in Inform. Theory, IT-17, p. 693, 1971.

7. Special Issue on Adaptive Antennas, IEEE Trans. on Antennas and Propagation, Vol. AP-24, No. 5, September 1976.
8. S. Lang, "Performance of maximum entropy spectral estimators", SM Thesis MIT Electrical Engineering Dept., May 1979.
9. S. Lang, "Near optimal frequency/angle of arrival estimates based on maximum entropy spectral techniques" in Proc. 1980 IEEE Int. Conf. on Acoustics, Speech and Signal Processing, pp. 829-832, 1980.
10. T.J. Ulrych and R.W. Clayton, "Time Series Modelling and Maximum Entropy", Phys. Earth and Planet. Inter., Vol. 12, pp 188-200, 1976.
11. J. Makhoul, "Linear prediction: a tutorial review" Proc. IEEE, Vol. 63, pp. 561-580, April 1975.
12. J. R. Sklar and F.C. Scheppe, "The Angular Resolution of Multiple Targets", Lincoln Laboratory Group Report 1964-2, January 1964.
13. W.D. White, "Angular spectra in radar applications" IEEE Trans. on Aerospace and Electronic Systems, AES-15, pp. 895-899, Nov. 1979.
14. D. Childers (editor), Modern Spectrum Analysis. IEEE Press, N.Y., 1978.
15. J. Evans, "Aperture sampling techniques for precision direction finding" in ELECTRO 78 Record, May 1978, also IEEE Trans. on Aerospace, pp. 891-895 Nov. 1979.
16. J. Capon, "Multipath Parameter Computations for the MLS Simulation Computer Program", M.I.T. Lincoln Laboratory Project Report ATC-68, FAA-RD-76-55, 1976.
17. J. Evans, D. Sun, S. Dolinar, D. Shnidman, "MLS Multipath Studies, Phase 3 Final Report, Volume I: Overview and Propagation Model Validation/Refinement Studies", M.I.T. Lincoln Laboratory Project Report ATC-88 (1979).

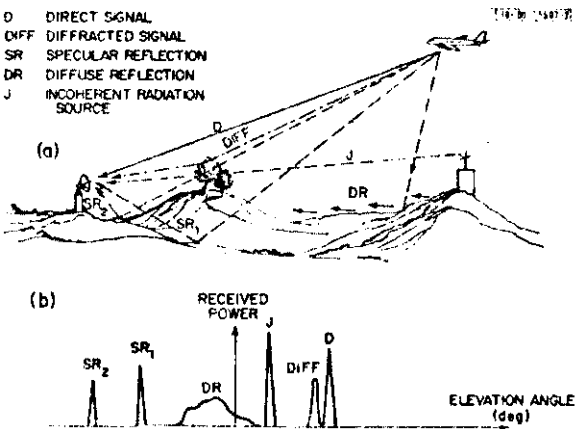


Fig. 1-1. (a) Multipath propagation phenomena of interest. (b) Relationship of received power to low-angle multipath environment.

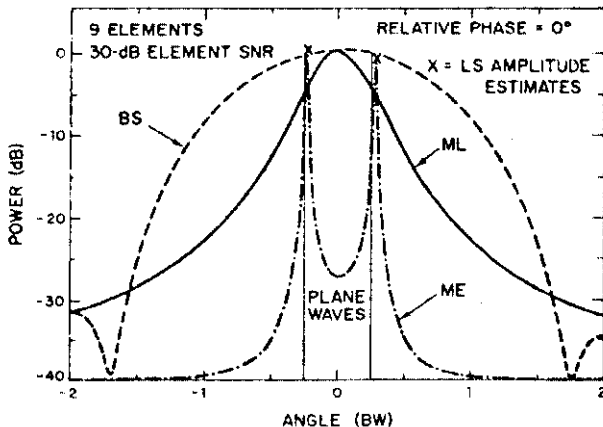


Fig. 2-1. Synthetic Data: two plane waves at 0.5 BW separation.

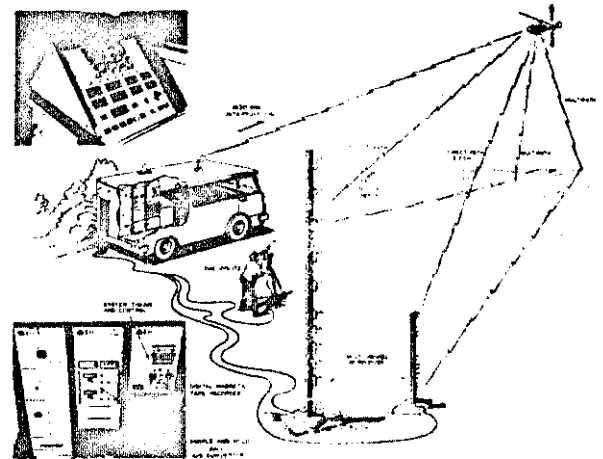


Fig. 3-1. Terrain multipath experimental configuration.

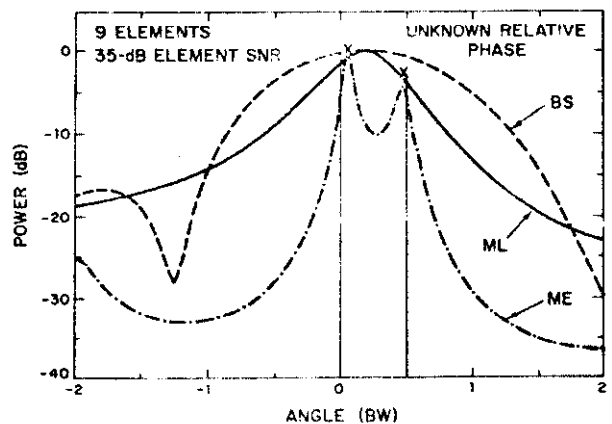


Fig. 3-2. Antenna Test Range Measurement: two signals at 0.5 BW separation.

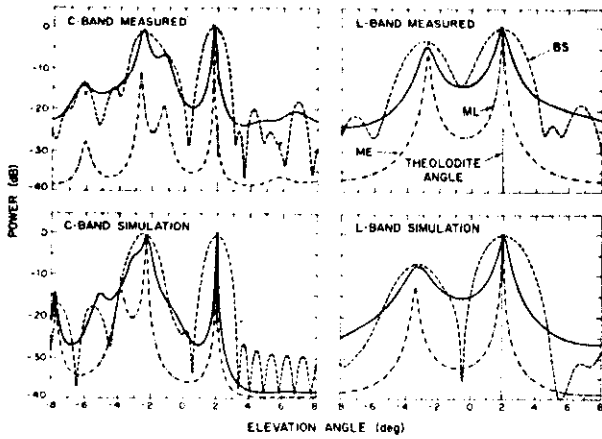


Fig. 3-3. Hanscom AFB measurement: near-flat terrain.

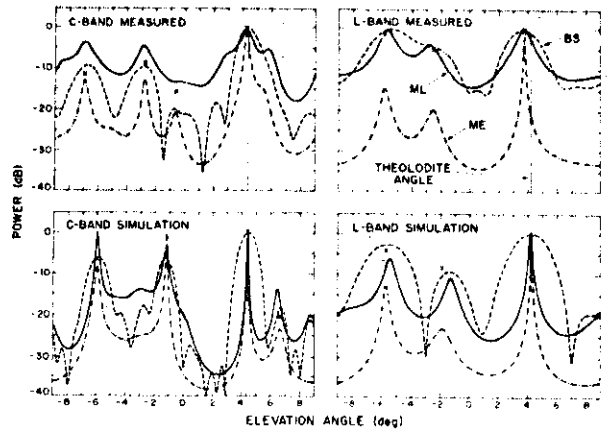


Fig. 3-5. Fort Devens golf course measurement: rolling terrain.

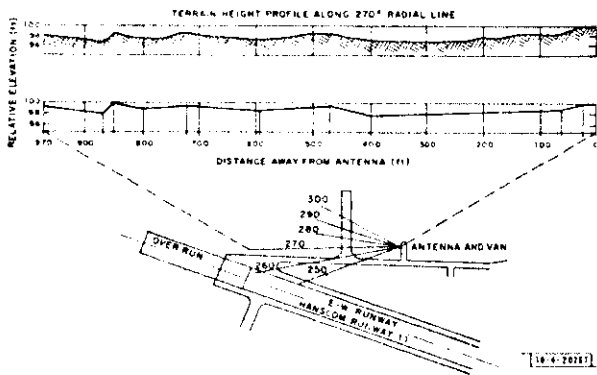


Fig. 3-4. Terrain height profile at Hanscom AFB: near-flat terrain.

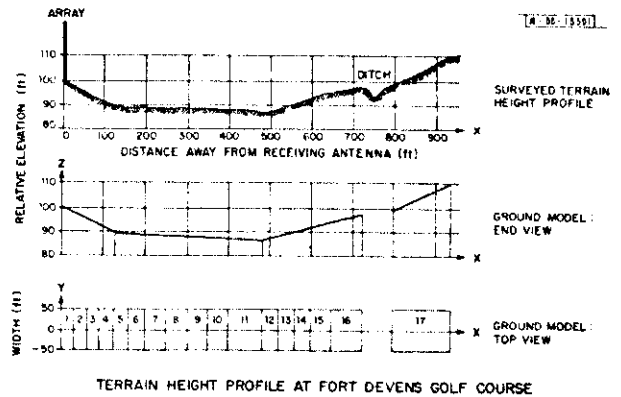


Fig. 3-6. Terrain height profile at golf course of Fort Devens: rolling terrain.